Coherent pulse propagation through resonant media

U. van Bürck

Physik-Department E15, Technische Universität München, D-85748 Garching, Germany

Resonant pulse propagation (RPP) is reviewed with special emphasis on the propagation of synchrotron radiation (SR) pulses through nuclear single-resonance media. The most remarkable feature in the time evolution of RPP is the dynamical beat (DB), a pronounced modulation with periods increasing with time and decreasing with increasing sample thickness. A comparison of RPP at γ-wavelengths (SR and Mössbauer radiation) with RPP in the infrared and visible regimes in case of molecular, atomic and excitonic resonances reveals an astonishing universality of the observed phenomena. The DB is described within the double-hump picture and the group-velocity picture, and is finally attributed to the energy exchange between radiation field and oscillator system in multiple scattering.

1. Introduction

Nuclear forward scattering (NFS) of synchrotron radiation (SR) can be considered as the time–domain coherent scattering variant of classical Mössbauer spectroscopy. In NFSSR the nuclear sample is excited by a short, broadband SR flash, and the subsequent free decay of the nuclear excitation is observed. In forward scattering the contributions of all nuclei are spatially in phase and interfere constructively. The time evolution of this coherent signal contains information about the nuclear resonance and the hyperfine interactions of interest (for a review see, e.g., [1,2]).

The initial NFSSR intensity at time zero depends $\propto T^2$ on the effective thickness T of the sample. In order to get an intense signal, samples of thickness $T \geqslant 1$ have to be employed, depending on available SR flux and beam time. In this thickness regime, however, multiple scattering becomes important and determines the propagation of the radiation pulse through the sample. Thus the time evolution of NFSSR does not follow a natural exponential decay as expected in the single-scattering approximation, but exhibits pronounced intensity modulations characteristic of coherent resonant pulse propagation (RPP). Therefore the interpretation and evaluation of practically any investigation based on NFSSR requires knowledge about RPP. RPP means in the following the propagation of pulses with bandwidth large enough to cover the entire resonance.

RPP was first considered theoretically at the begin of this century by Sommerfeld and Brillouin [3] in connection with questions about signal velocity and the theory of relativity. With the advent of the Mössbauer effect in the late fifties, experiments on RPP in case of nuclear resonances became feasible, and the study of RPP of Mössbauer

γ-radiation was initiated by the theoretical and experimental work of Lynch et al. [4]. Later on the field got a new impetus in the eighties by the realization of nuclear resonant scattering of pulsed SR by Gerdau et al. [5]. The short, broadband excitation of the nuclear system facilitated the observation of coherent transient effects. Already in the first observation of NFSSR by Hastings et al. [6] a pronounced intensity modulation due to multiple scattering was revealed in the time evolution of the collective nuclear decay as predicted by Kagan et al. [7].

This, however, was not the first observation of strong effects of RPP. In the infrared and visible regions, the study of transient phenomena had become possible with the advent of the laser. Besides the main studies concerned with nonlinear effects observed with high-intensity laser pulses, also the linear interactions of low-intensity pulses were investigated. Propagation of low-intensity laser pulses was studied at first theoretically in the late sixties by Burnham and Chiao [8] and Crisp [9]. With the introduction of laser pulses in the picosecond regime, broadband excitation of optical resonances was facilitated, and pronounced effects of RPP were revealed in experiments and compared with theory in the case of molecular resonances in the infrared by Hartmann and Laubereau [10], and in the case of atomic resonances in the visible by Rothenberg et al. [11]. Later, similar effects were observed also in the case of excitonic resonances, for free excitons by Fröhlich et al. [12], for bound excitons by Jütte et al. [13], and for excitons in quantum well structures by Kim et al. [14]. A first demonstration of RPP effects in the case of phononic resonances was reported by Bakker et al. [15]. The wide use of sub-picosecond laser technology in recent years implies to an increasing degree the impulsive, broadband excitation of the resonances under study. Thus, as in NFSSR, RPP plays an important role in modern coherent laser spectroscopy.

The aim of the present paper is to convey an understanding of the basic phenomena observed in pulse propagation through a medium which exhibits a single nuclear resonance. For this purpose, the theoretical and experimental results for resonant propagation of γ-ray and light pulses will be briefly reviewed in sections 2 and 3. Based on this material, the main features of RPP will be discussed and interpreted in section 4. In section 5 the universality of the observed phenomena will be pointed out, and possibilities of mutual stimulation between the two regimes of RPP at visible and γ-radiation wavelengths will be discussed. Throughout the paper, RPP will be considered mainly in the linear regime, where the induced polarization follows linearly the exciting radiation field, and for radiation pulses of very low intensity, where the ground state population remains unchanged (weak small-area pulses [9,11,16]). The present paper is based on considerations previously presented in [17].

2. Theoretical results

2.1. The Sommerfeld and Brillouin precursors

Sommerfeld and Brillouin [3] have investigated the propagation of a truncated harmonic wave through a strongly dispersive medium. Their work is considered as

basic in the field of signal transmission and has entered classical textbooks [18]. In the last twenty years, the topic has been taken up again and extensively studied mainly by Oughstun et al. (see [19] and references therein). A short summary of the original work in modern terms can be found in [20].

Let the interaction of the electromagnetic radiation with the resonant medium be described by a refractive index $n(\omega)$ given by

$$n^2(\omega) = 1 - \frac{a^2}{\omega^2 - \omega_0^2 - \mathrm{i}\omega\Gamma_0/\hbar}, \tag{2.1}$$

where ω is the frequency of the radiation, ω_0 the frequency and Γ_0 the full energy width at half maximum of the resonance of a system of harmonic oscillators. The parameter a^2 describes the coherent scattering strength of the oscillators, which can be defined either off resonance or in resonance. In the off-resonance definition, which is frequently used in atomic resonant scattering by electrons, a is equal to the plasma frequency ω_p [8,18] or in quantum-optical terms $a^2 = 4c\alpha_0$, with c the light velocity and α_0 a constant related to the square of the dipole matrix element [9,16,48]. In the in-resonance definition, a^2 is expressed via μ_r, the absorption coefficient at resonance: $a^2 = \mu_\mathrm{r} c\Gamma_0/\hbar = (T/d)c\Gamma_0/\hbar$. In nuclear resonant scattering the effective thickness T (or optical thickness at resonance, $T = \beta$ [4] $= 4\xi$ [7]) has become customary, where $T = \mu_\mathrm{r} d = \sigma_0 f_\mathrm{LM} \eta N d$, with d the sample thickness, σ_0 the nuclear cross-section, f_LM the Lamb–Mössbauer factor, η the isotopic enrichment, and N the density of nuclei. The coherent scattering strength of the oscillators is thus given in the in-resonance definition by c times the absorption area $\mu_\mathrm{r}\Gamma_0/\hbar$. The two definitions of the parameter a^2 are in agreement with the Kramers–Kronig sum rule $\omega_\mathrm{p}^2 = -(2/\pi)\int_0^\infty \omega \mathrm{Im} n^2(\omega)\,\mathrm{d}\omega$ [18].

The result of Sommerfeld and Brillouin is essentially that at the depth d in the medium two forerunners of the signal are observed. The Sommerfeld precursor, corresponding to the excitation of the high-frequency branch of the dispersion relation for the wavevector $k(\omega) = n(\omega)\omega/c$, arrives at time d/c, with frequency decreasing with time. At time $(d/c)\sqrt{1 + a^2/\omega_0^2}$ the Brillouin precursor arrives, corresponding to excitation of the low frequency branch, with frequency increasing in time.

2.2. Dynamical beat and speed-up of the initial decay

For the calculation of NFS of Mössbauer radiation, Lynch, Holland and Hamermesh have applied linear response theory. In this approach the incident pulse is decomposed into its frequency components, the refraction during transmission through the sample is calculated for each frequency component, and the time evolution of the outgoing pulse is obtained by Fourier transformation. This way they derived for the transmission of Mössbauer radiation from a radioactive source with Lorentzian energy distribution of width Γ_0 (corresponding to an exponential decay with lifetime $t_0 = \hbar/\Gamma_0$), when it is tuned to resonance of a sample of the same width Γ_0 and of

effective thickness T, the following law for the time evolution of the transmitted pulse envelope [4]:

$$E(t) \propto \mathrm{e}^{-\tau/2} J_0\big(\sqrt{T\tau}\,\big), \tag{2.2}$$

where $\tau = t/t_0$ and J_0 is the Bessel function of first kind and order zero. The time t is henceforth counted from the arrival of the prompt pulse front at the detector. If source and sample resonance do not coincide, a solution involving an infinite series of Bessel functions has been found instead. The results of this classical calculation have later been confirmed in a quantum-mechanical derivation by Harris [21].

By the same classical method the corresponding law for the delayed transmission of an incident δt-pulse of broadband SR was obtained by Kagan et al. [7]:

$$E(t) \propto T\mathrm{e}^{-\tau/2} \frac{J_1\big(\sqrt{T\tau}\,\big)}{\sqrt{T\tau}}, \tag{2.3}$$

where J_1 is the Bessel function of first kind and first order. For $\tau < 1/(1+T/4)$, i.e., for very thin samples or for very early times, expansion of eq. (2.3) yields [22]

$$E(t) \propto T\mathrm{e}^{-(1+T/4)(\tau/2)}. \tag{2.4}$$

These equations give in short form the main results of RPP in case of nuclear resonant scattering. Equations (2.2) and (2.3) describe the *dynamical beat* (DB) in NFS of Mössbauer radiation and of SR, respectively. Equation (2.4) describes the *speed-up of the initial decay* in NFSSR. Details of these solutions will be discussed in connection with the experimental results presented in section 3.3.

Such closed analytical solutions can only be derived for the ideal case of a single-line resonance. But also in the case when the hyperfine splitting is large in comparison with the resonance linewidths slightly modified closed solutions can be used [22,23].

2.3. Alternative derivations

The transmission of laser radiation through matter is in general described by the coupled Maxwell and optical Bloch equations [16]. Crisp [9] has shown that for low intensity pulses with small area the equations can be linearized and further simplified if a Lorentzian frequency distribution is assumed for the resonance. For the special case of an incident δt-pulse a law identical with the one given in eq. (2.3) has been obtained via Fourier transformation (eq. (33) in [9]).

Another very illustrative derivation for the special case $t_0 = \infty$ has been given by Burnham and Chiao [8]. For boundary conditions corresponding to an incident δt-pulse, they simultaneously solve Maxwell's wave equation and the harmonic oscillator equation. Staying in the time domain, they obtain via the Bessel differential equation of order zero a solution corresponding to the one given by eq. (2.3) (eq. (20b) in [8]). A time–domain derivation of the exact solution including a finite lifetime t_0 has later been given by Laubereau and Kaiser [24].

When comparing these solutions from different fields of radiation physics, the reader should be aware of different definitions of the parameter a^2 of eq. (2.1). In nuclear resonance scattering of γ-radiation it is natural to use the in-resonance definition, where the argument under the square roots in eqs. (2.2) and (2.3) becomes $T\tau$. A similar notation was employed in case of molecular resonance scattering in [24, eq. (90)]. In atomic resonance scattering of visible radiation, by contrast, the off-resonance definition of the parameter a^2 is used, where the argument under the square root of the Bessel function becomes $(\omega_p^2/c)td$ [8] or $4\alpha_0 td$ [9]. Also note that the definitions of the characteristic decay or dephasing times used by different authors may differ by a factor of 2.

In NFS of Mössbauer radiation and of SR different forms of solutions were recently obtained by Ruby [25] and Hoy [26] starting from a microscopic picture, where the multiple scattering paths were calculated explicitly. The resulting solutions [26] for thick absorbers approximately correspond to the exact solutions eqs. (2.2) and (2.3) with the relevant Bessel functions being expanded in series.

In practice, however, experimental results are usually analyzed using numerical solutions. Such calculations are either performed in the frequency space, based on eq. (2.1), with the time evolution finally obtained by Fourier transformation, or directly in the time domain. Here the single-line Lorentzian approach of Burnham and Chiao [8] has lately been essentially extended by Shvyd'ko to solve in a general way more complicated cases in nuclear resonant scattering [27]. His treatment yields an iterative solution in time and space, which is quite flexible and also well suited to compute NFS time evolutions under the influence of timed perturbations.

Numerical solutions have to be used whenever several near-neighbouring resonances, e.g., caused by small hyperfine splitting, are coherently excited. Furthermore, in the case of laser pulses the δt-pulse approximation is not exact. Also, for free excitons, spatial dispersion necessitates an additional term $\omega_0 \hbar k^2/M$ in the denominator of eq. (2.1) related to the kinetic energy of an exciton with finite mass M [12]. Nevertheless, it will be seen that these complications have rather little effect, so that the different cases of RPP can be compared and understood on the basis of eqs. (2.2)–(2.4).

3. Experimental results

3.1. Observation of precursors

The precursors predicted by Sommerfeld and Brillouin [3] rely on the transmission of radiation components off resonance. Thus whenever radiation with a broad frequency content is incident, e.g., in the case of exponentially decaying pulses or SR, prompt contributions arriving with light velocity can be observed and interpreted as Sommerfeld–Brillouin precursors [28,29]. The decisive point is whether the Sommerfeld and Brillouin precursors can be separated and identified. So far this has only been possible in the case of microwave radiation [20]. According to the discussion following eq. (2.1), the separation between the two precursors is given by $\Delta t \approx T\Gamma_0/2\omega_0^2\hbar$. For

broad resonances of low frequency this delay is measurable. For the ^{57}Fe Mössbauer resonance, however, Δt is of order 10^{-30} s, and the two precursors practically coincide in time.

3.2. Mössbauer radiation and nuclear resonances

In Mössbauer spectroscopy, the time evolution of the radiation emitted from a radioactive source and transmitted through a nuclear resonant absorber can be measured when the signal of the preceding decay leading to the excited Mössbauer level is used as time zero, e.g., in case of ^{57}Fe the 122 keV signal coincident with the population of the 14.4 keV level.

The pronounced DB described by eq. (2.2) has so far hardly been observed in such time-correlation experiments for resonant Mössbauer radiation, neither for hyperfine split resonances [4] nor for a single line resonance [30]. The reason is the strong absorption at resonance, which makes the transmitted signal largely dominated by recoil radiation, which is inelastically emitted by the source and does not interact with the sample. The strong resonance absorption can only be avoided by slightly detuning source and resonant sample.

In this way, pronounced oscillations have been observed in the transmitted signal depending on sample thickness and on detuning [4,28,30,31]. They can be well fitted using the original theory of Lynch, Holland and Hamermesh, thus proving the validity of their approach [4]. However, the oscillations seem to be more due to detuning than to RPP since their frequency increases with the energy distance from resonance. In principle the same effects are observed in time-slicing (time-filtering) Mössbauer spectroscopy, where in Mössbauer spectra recorded during a certain delayed time window pronounced oscillations around resonance appear [4,32] (for later work see, e.g., [33] and references therein).

Expansion of eq. (2.2) for small values of $T\tau$ yields an exponential decay law $E(t) \propto \mathrm{e}^{-(1+(T/2))(\tau/2)}$, describing a speed-up of the initial decay twice larger than for NFSSR. In spite of the intense background due to recoil radiation, a speed-up of the initial decay increasing with thickness T has indeed been observed in time-correlation experiments for resonant Mössbauer radiation transmitted through foils of different thicknesses [4,30].

Another type of timing measurements can be performed in Mössbauer spectroscopy when the time evolution of the intensity in the forward direction is observed after a fast external perturbation of the relation between source and absorber. Such perturbations have for instance been produced by rapid passage through resonance (see, e.g., [34] and references therein), stepwise phase switching (see [35] and references therein), stepwise energy switching [36], or by shuttering [37]. In all these cases coherent transients have been observed, for the detailed analysis of which it was found necessary to take into account multiple forward scattering. But again, except for a speed-up of the initial decay, effects of RPP were difficult to identify against the background of recoil radiation from the source.

3.3. Synchrotron radiation and nuclear resonances

In NFSSR, the sample is excited by a short SR pulse of some hundred picoseconds duration, determined by the spread of the electron bunch, and of several meV bandwidth, determined by the high-resolution monochromator. This bandwidth exceeds the nuclear resonance widths by five to six orders of magnitude. NFSSR is almost free of background, and so the visibility of its time evolution depends only on SR intensity and available time window.

Already in the first demonstration of NFSSR, a pronounced DB has been observed [6]. By the appropriate choice of the magnetization, only the two $\Delta m = 0$ transitions of the ^{57}Fe metal sample foils were excited in this experiment, so that the hyperfine splitting was large in comparison with the resonance width. In this case the DB is revealed as an envelope modulation over the fast quantum beat (QB) resulting from hyperfine splitting [22,23,38,39]. A typical spectrum is shown in figure 1. In case of hyperfine splitting, the total effective thickness T is distributed into partial thicknesses T_p according to the different hyperfine transitions. Since the sample of figure 1 has the same partial thickness $T_\mathrm{p} = T/2$ for both Δm = 0 hyperfine transitions, the dynamical beats connected with these transitions coincide. The thickness dependence of the speed-up of the initial decay and of the DB were studied for the resonant transmission of SR pulses through ^{57}Fe metal foils in the ranges $T_\mathrm{p} \approx$ 4–25 and $T_\mathrm{p} \approx$ 72–216, respectively [22]. For one of these foils the temperature dependence of NFSSR in the range of 10–1048 K was also measured, with particular attention paid

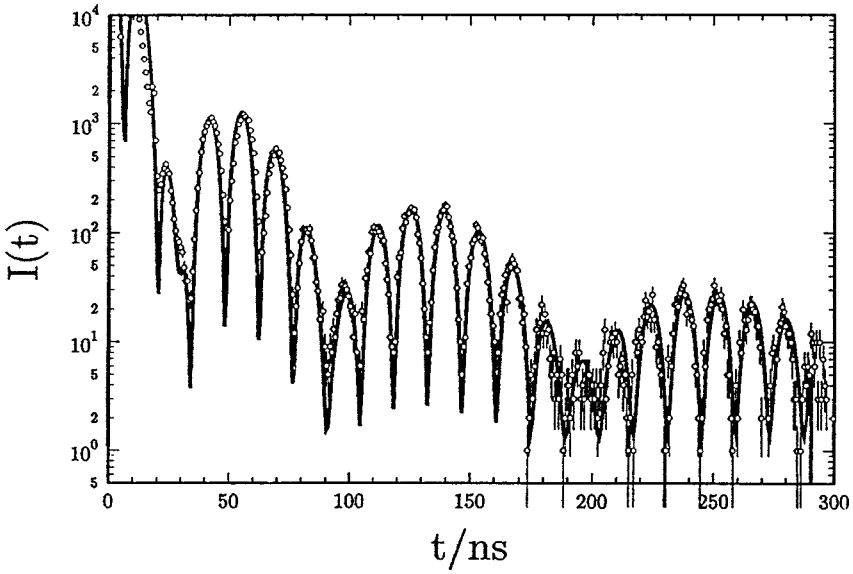

Figure 1. Time evolution of NFSSR through $a \approx 9$ μm ^{57}Fe metal foil at 4 K in a vertical magnetic field of 1 T [23]. Only the two $\Delta m = 0$ transitions were excited, with effective thickness $T_\mathrm{p} \approx 75$ each. The DB is seen as an envelope modulation over the fast QB. The solid lines are fits using the NFS theory via Motif [83].

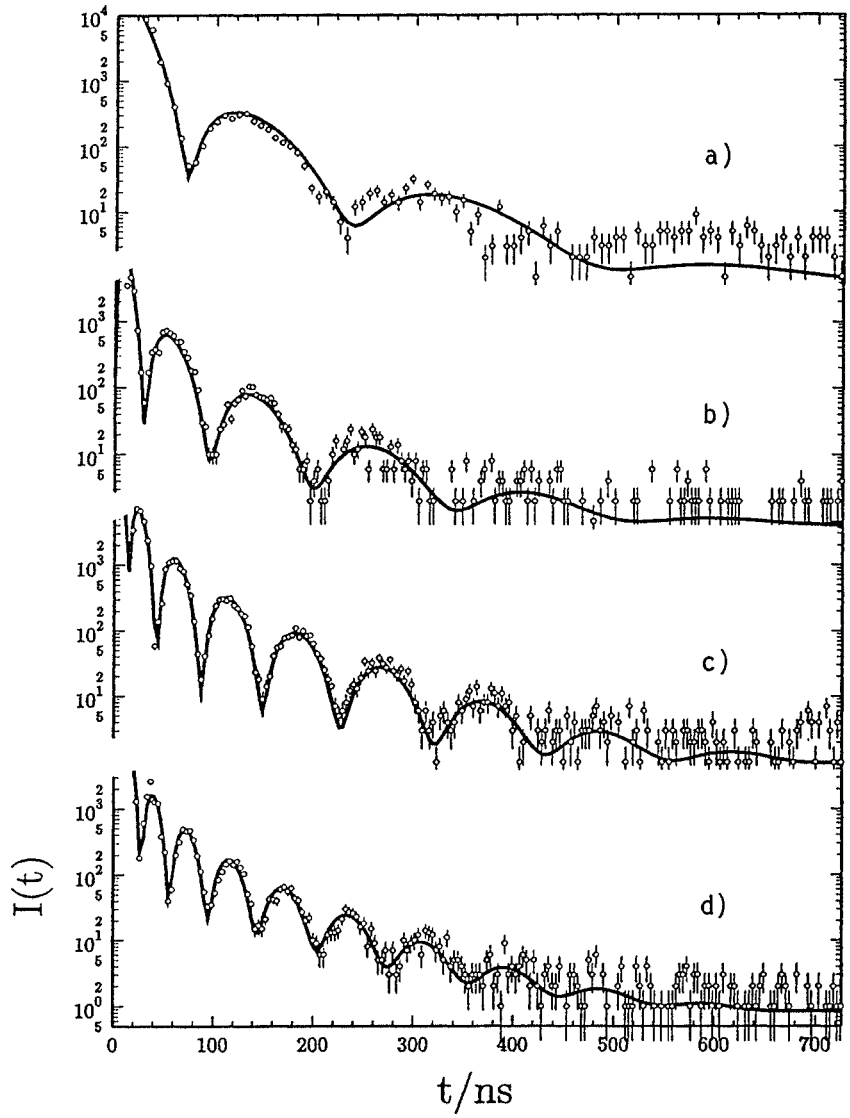

Figure 2. Time evolution of NFSSR through enriched SS metal foils of different effective thicknesses $T \approx 35$ (a), 90 (b), 210 (c), and 330 (d) [41]. The aperiodic modulation is the DB, with apparent periods increasing with time and decreasing with increasing effective thickness. The solid lines are fits using the NFS theory via Motif [83].

to effects due to the decrease of the Lamb–Mössbauer factor and the decrease of the hyperfine splitting [39].

In order to investigate a pure DB without disturbance by a QB, single-line materials were employed. RPP was studied for stainless steel (SS) metal foils of composition $^{57}Fe_{55}Cr_{25}Ni_{20}$ in the ranges $T \approx 18$–290 [40] and $T \approx 35$–330 [41]. Figure 2 shows as an example the thickness dependence of the DB for SS foils in a relatively large

time window [41]. A similar thickness dependence was observed for powder samples of $(NH_4)_2Mg\,^{57}Fe(CN)_6$ in the range $T \approx 20$–400 [42], which is displayed in figure 3. This compound is equivalent to the standard Mössbauer single-line material $K_4\,^{57}Fe(CN)_6$ with the potassium replaced by light elements in order to reduce the electronic absorption. In figures 2 and 3 two characteristic features of the DB can be noticed:

1. The DB is aperiodic, the apparent periods increase with time.

2. The apparent DB periods decrease with increasing sample thickness.

The slope of the initial decay cannot be seen so well from these figures because of detector overload and veto in the electronic circuit for the first 10–20 ns. For this reason the thickness dependence of NFSSR studied with thin ^{57}Fe metal foils in the range $T_{\mathrm{p}} \approx 4$–25 [22] is reproduced in figure 4. It demonstrates the following feature:

3. The initial decay is sped up proportionally to sample thickness.

For the identification of the observed beat signal it is of importance to determine not only the intensities, but also the phases. For this purpose the NFS signals of samples of different thicknesses have to be brought to interference. This was accomplished by spatial beam separation and recombination in an LLL-interferometer [43] and by energy separation in the direct beam either due to constant velocity motion [44] or by ultrasound excitation [45] of one of the samples. As an example, the time evolution of NFSSR through two SS foils is shown in figure 5, where one foil was moved at constant velocity of ± 18 mm/s [44]. When two foils of 1.5 μm thickness each are employed, their NFS signals are identical and a regular QB is observed. However, when one of the foils is replaced by a foil of 10 μm thickness, phase jumps of π are recognized in the QB at $\sim$25 and 84 ns, indicating sign changes of the NFS amplitude of the thicker foil. The phase jumps of π occur at the zeroes of the DB modulation of the thicker foil and demonstrate the fourth characteristic of the DB:

4. The field amplitude of the DB changes sign at every beat.

These four characteristic features are in complete quantitative agreement with the theoretical predictions given by eqs. (2.3) and (2.4). Qualitatively, it can directly be seen that the increase of the apparent beat period with time corresponds to the fact that the normalized time τ does not appear linearly but rather as $\sqrt{\tau}$ in the argument of the Bessel function J_1. Note also that the asymptotic expression of the Bessel function J_1 for large arguments exhibits a similar oscillation $\propto \cos(\sqrt{T\tau} - 3\pi/4)$ with period increasing in time [7]. The decrease of the apparent beat period with increasing thickness T is reflected by the dependence of the Bessel function on $\sqrt{T\tau}$, i.e., on the product of T and τ. The speed-up of the initial decay proportional to thickness T and the oscillatory behaviour of the field envelope $\propto J_1$ with sign changes at every beat are also directly obvious from eqs. (2.3) and (2.4).

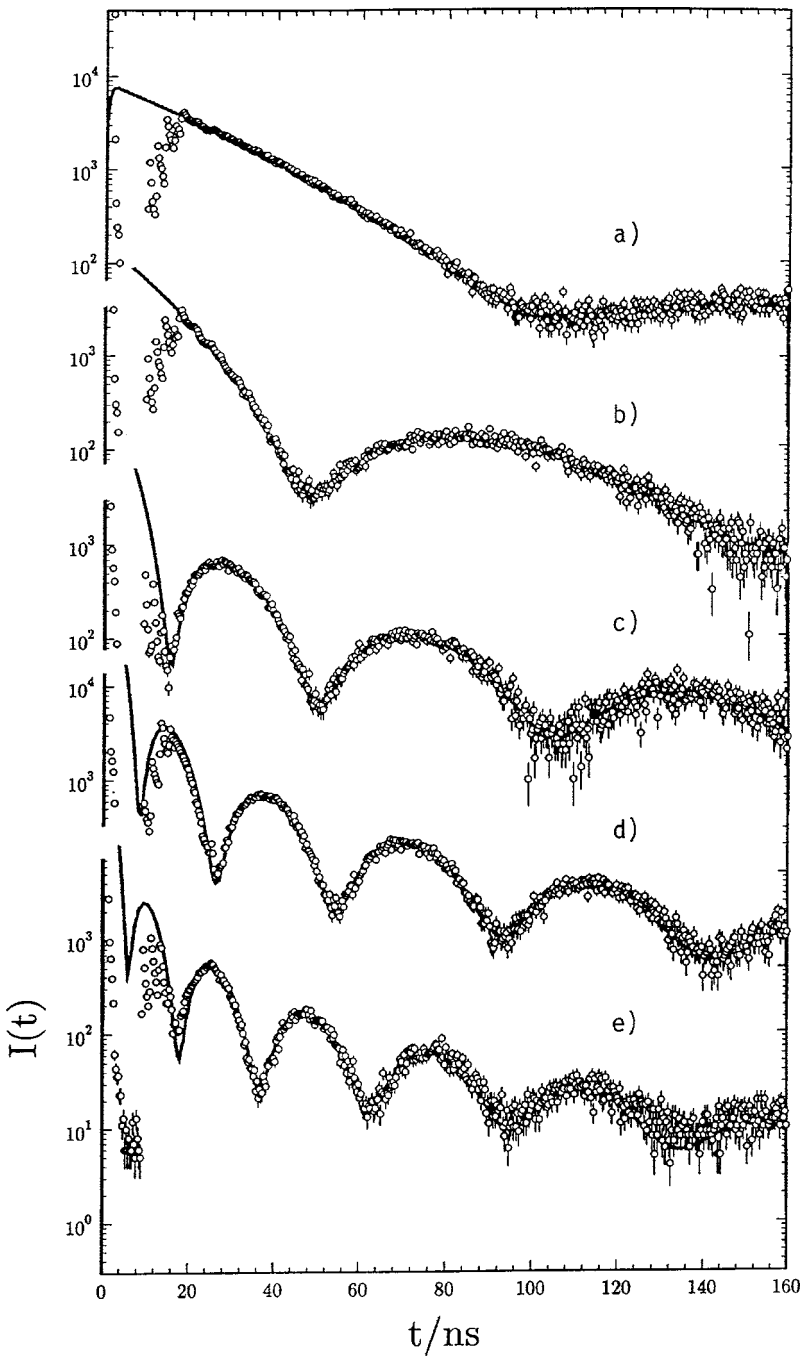

Figure 3. Time evolution of NFSSR through $(NH_4)_2Mg^{57}Fe(CN)_6$ powder samples of different effective thicknesses $T \approx 20$ (a), 44 (b), 140 (c), 275 (d), and 408 (e) [42]. The aperiodic modulation is the DB. The solid lines are fits using the NFS theory via Motif [83].

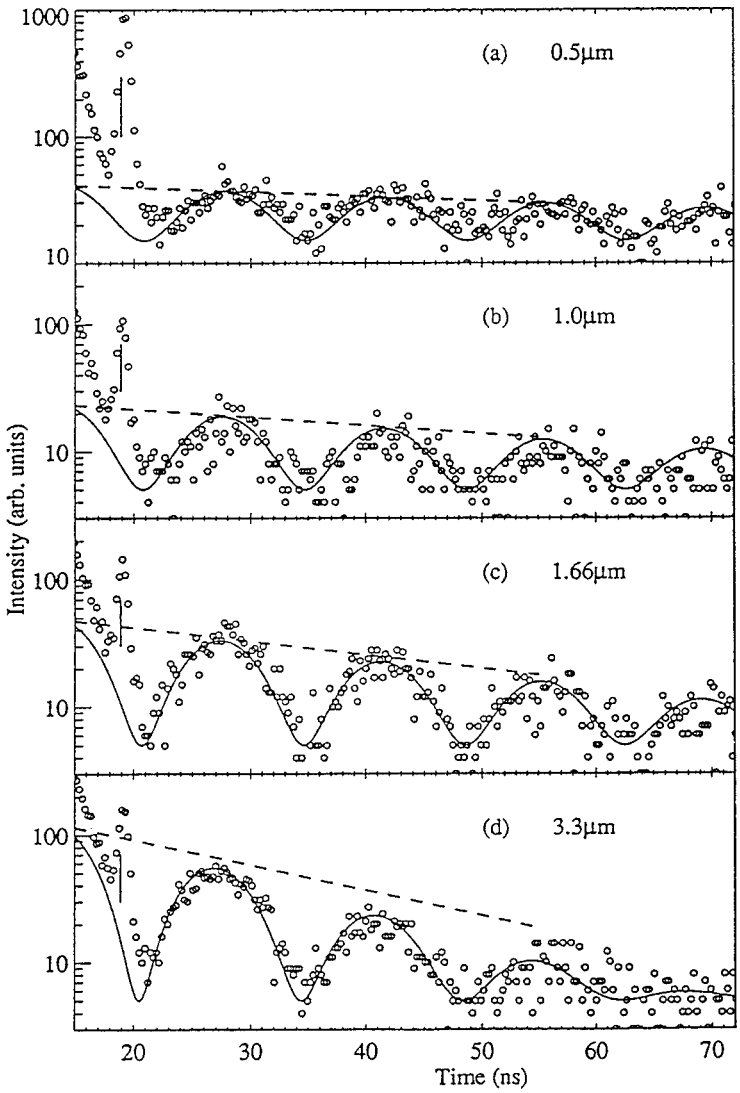

Figure 4. Time evolution of NFSSR through ^{57}Fe metal foils of different effective thicknesses in a vertical magnetic field [22]. Only the two $\Delta m = 0$ transitions were excited, with effective thicknesses $T_p \approx 4$ (a), 8 (b), 13 (c), and 25 (d). The solid lines are computations based on eq. (2.3). The dashed lines indicate the exponential decay of the envelope as calculated using eq. (2.4).

As a result, we can say that the compact solutions eqs. (2.3) and (2.4) fully describe the effects of RPP observed in NFSSR in case of single or well separated resonance lines. In many cases, however, the sample is not of single-line material, nor is the hyperfine splitting large in comparison with the linewidths. In these cases the effects of RPP and interresonance interference merge, and DB and QB melt into hybrid forms of beating [23,46,47].

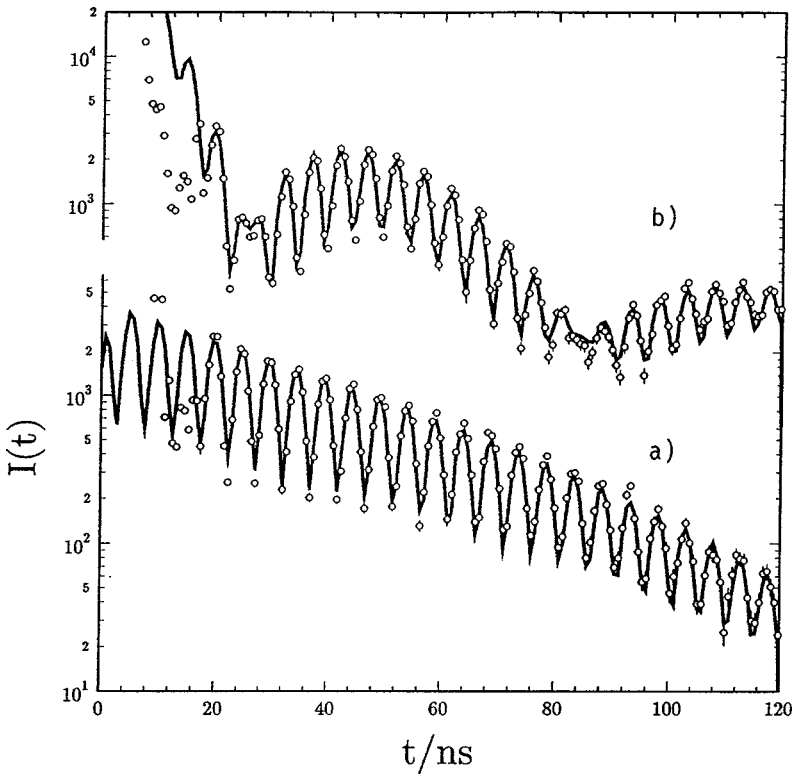

Figure 5. Time evolution of NFSSR through two enriched SS metal foils moving at a constant velocity of ± 18 mm/s with respect to each other, for two foils of 1.5 μm thickness each (a), and for two foils of 10 and 1.5 μm (b) [44]. The time evolution in spectrum (a) exhibits a regular QB. By contrast, the QB in time spectrum (b) shows phase jumps of π at $\approx$25 and 84 ns. At these times the envelope of the scattering by the 10 μm foil alone passes through the first two zeroes of the Bessel function J_1. The solid lines are fits using the NFS theory via Motif [83].

3.4. Laser radiation and molecular, atomic and excitonic resonances

In almost any timing experiment in the field of coherent laser spectroscopy transient effects have been observed as soon as the bandwidth of the incident pulse reached or exceeded the width of the resonance. With the spread of sub-picosecond laser technology this now happens frequently. With ratios of bandwidth to resonance width up to four orders of magnitude [48] even the conditions of impulsive excitation prevailing in NFSSR have practically been reached. The observed beat phenomena, called propagation beat [77] or polariton beat [12,13,49,50] in the case of excitonic resonances, almost follow the DB defined by eq. (2.3). In the following we want to point out those experiments where the characteristic features of RPP have been revealed most clearly.

(a) Aperiodicity of the beat. Pronounced aperiodic beats with periods increasing in time have been observed for the transmission of picosecond laser pulses tuned to atomic [11] and excitonic [12] resonances. As an example, a polariton beat measured

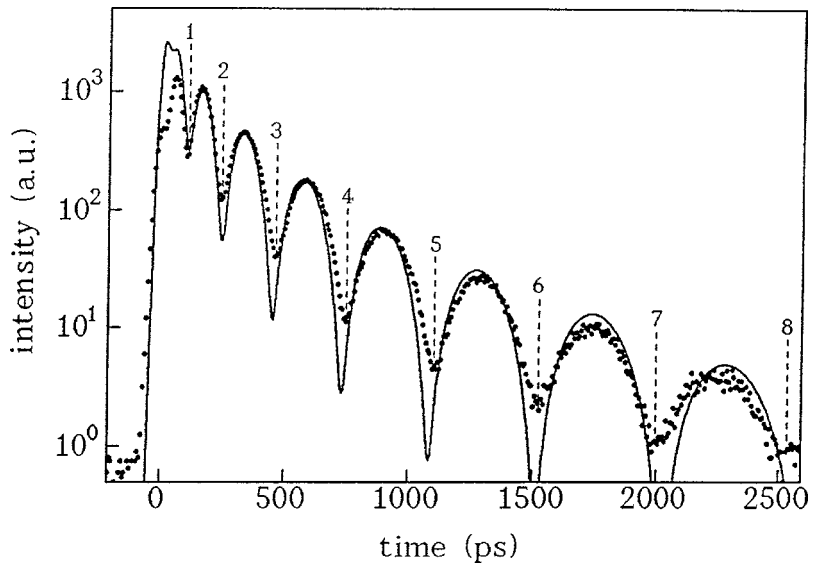

Figure 6. Time evolution of the transmission of 30 ps laser pulses through a Cu_2O single crystal exhibiting a free exciton resonance at 2 eV [12]. The solid line denotes the numerical calculation. The numbered minima of the propagation beat almost coincide with those of a DB as given by eq. (2.3) for optical thickness $T \approx 250$ and lifetime $t_0 \approx 1$ ns.

at thickness $T \approx 250$ is reproduced in figure 6 [12]. Here the observation of the beat over a time window of more than 2 ns was facilitated by the long lifetime and dephasing time of the polariton in the case of a dipole forbidden exciton resonance in Cu_2O. The beat of figure 6 differs only slightly from a DB as given by eq. (2.3). The differences have to be attributed to the finite ratio of pulse width to resonance width ($\approx$30) and to spatial dispersion due to a finite exciton mass. Later, aperiodic beats with increasing periods were reported in studies of RPP for an atomic resonance on a femtosecond scale [48] and for excitonic systems on pico- and femtosecond scales [13,49,50]. These measurements represent beautiful examples of ultrafast RPP dynamics.

(b) Thickness dependence of the beat. The thickness dependence of the beat was demonstrated with laser pulses tuned to atomic resonances in metal vapors of different densities in the ranges $T \approx$ 20–400 [11] and $T \approx$ 0.8–18 000 [48] as well as for an excitonic resonance in the range $T \approx$ 280–430 [50]. As an example for ultrafast pulse evolutions, the thickness dependence of the propagation beat on a femtosecond scale [48] is shown in figure 7. These results can be compared directly with those previously reported [11], where now optical thicknesses increased by approximately a factor 100 lead to 100 times faster propagation beats (compare figures 7(b) and (c) with [11, figures 2(c) and (e)], respectively). The correspondence of these two sets of pulse propagation data measured under quite different conditions is a convincing demonstration of the fact that the time evolution in RPP scales with the optical thick-

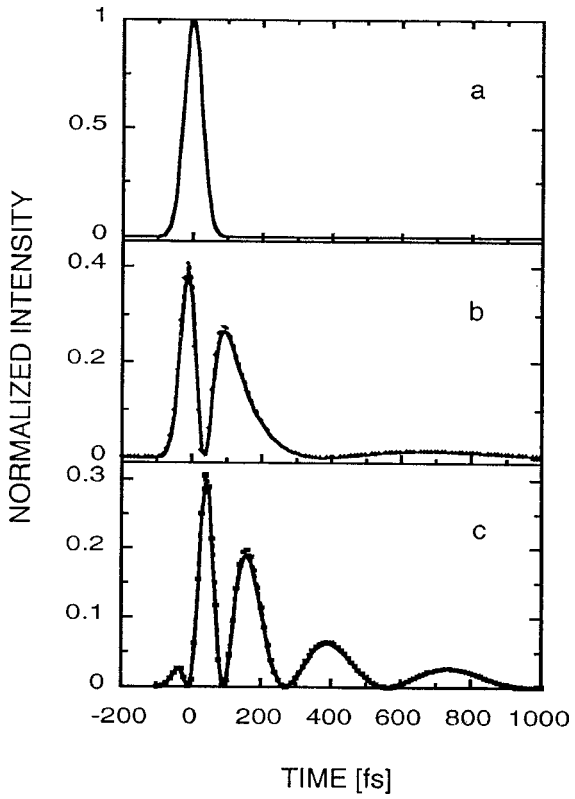

Figure 7. Time evolution of the transmission of 60 fs laser pulses through Cs vapor of different optical thicknesses $T \approx 0.8$ (a), 4000 (b), and 18000 (c) at the resonance energy of 1.46 eV [48]. The solid curves were derived from the experimentally observed autocorrelation traces, the dots represent theoretical calculations.

ness T. Also, the increase of the beat period with time is obvious from the spectra. The pulse evolutions observed in these measurements [11,48] also seem to correspond quite well and consistently to DB modulations as described by eq. (2.3), assuming lifetimes $t_0 \approx 100$ ps and optical thicknesses as given in the papers. Some minor features of the time evolutions, however, in particular the first intensity minimum at $\approx$40 fs in figure 7(b) or the minimum at 0 in figure 7(c), cannot simply be explained by DB modulations. These complications could be connected with the finite durations of the incident pulses (see figure 7(a) and [11, figure 2(a)], respectively).

(c) Thickness dependence of the initial decay. The thickness dependence of the speed-up of the initial decay is of special importance in coherent laser spectroscopy when relaxation times are to be determined from the free decay of the excitation. Here, for instance, the dependences of the relaxation or dephasing times on gas pressure have been studied in time–domain measurements for molecular gases [51,52] and for atomic vapors [53]. It was found that even in optically thin samples ($T \approx 1$) effects of RPP lead to significant distortions of the signals. For the determination of the

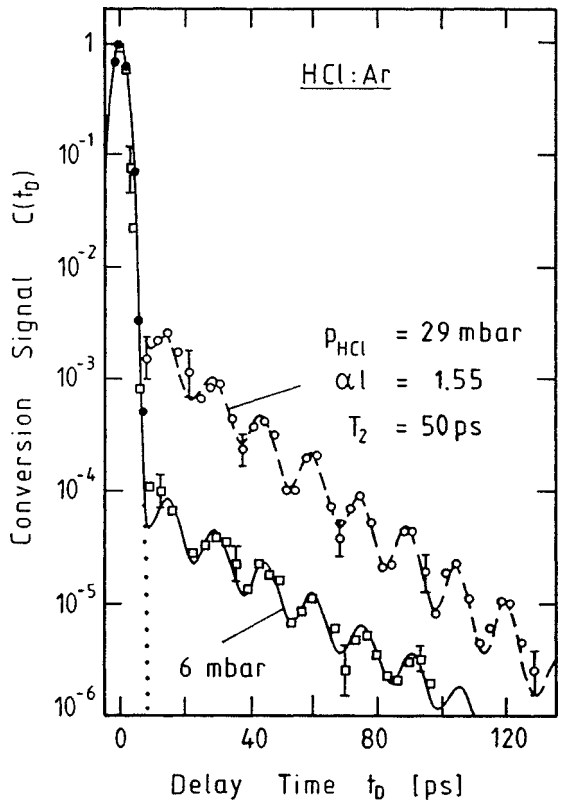

Figure 8. Time evolution of the transmission of 4 ps laser pulses through HCl with Ar buffer gas at the resonance energy of 0.37 eV [51]. The presence of two chlorine isotopes (75.5% ^{35}Cl and 24.5% ^{37}Cl) causes a line splitting of the vibration–rotation resonance, leading to the observed QB with period 15 ps. The lower (upper) curve corresponds to an optical thickness $T \approx 0.35$ (1.55). In the derivation of the dephasing times, the corrections for RPP given in [51] already amount to 8 and 20%, respectively, at these small optical thicknesses.

true relaxation times from the apparent forward scattering decay rates expressions equivalent to eq. (2.4) have been derived and have been verified experimentally [51–53]. An example for such measurements of the decay of the coherent forward scattering in optically thin samples [51] is shown in figure 8.

(d) Phase of the beat. The sign change of the field amplitude at the beat minima was revealed in the case of excitonic resonances in quantum well structures by Michelson interferometry, where the incident pulse was brought to interference with the resonantly transmitted pulse [14]. Phase jumps by π were also retrieved by a special Fourier transform method from time spectra measured around an excitonic resonance [13].

Thus, in all these studies employing laser radiation and resonances of quite different nature the same characteristic features have been revealed as observed for nuclear resonant propagation of SR pulses.

4. Interpretation of the characteristic features of RPP

For an intuitive understanding of the beat phenomenon in RPP sometimes the development of just the resonant frequency components of the pulse is discussed [9]. In this picture, the oscillators excited at resonance reemit with characteristic lifetime t_0 into the forward direction, where the reemission is in antiphase with respect to the incident pulse. The antiphase results from forward scattering at resonance (phase shift $\pi/2$) by a plane of scatterers (phase shift $\pi/2$). Incident and delayed forward scattered radiation form a pulse with inverted trailing edge [8,9]. When this pulse is scattered a second time, its trailing edge is again inverted with characteristic delay t_0, and so on. A serious failure of the picture, however, is that the beat phenomenon is not caused by the few radiation components at resonance, but mainly by the components in the wings off resonance, for which the phase shift is not π. The domination of the frequency wings in RPP becomes clear from the high intensities at early times and from the relatively weak absorption of the pulses. For this reason an explanation of the effects of RPP has to be searched for based on refraction around resonance rather than on absorption or scattering at exact resonance.

4.1. Double-hump picture

The time-integral energy distribution of NFSSR for optically thick samples shows a pronounced oscillatory behaviour around resonance, dominated by the contribution of the frequency wings below and above resonance. These off-resonance contributions form two peaks, often called double humps [2,54]. The double-hump distribution can be directly derived from a scattering phase diagram (see [2, figure 3]) and is quantitatively computed as $|1 - R(\omega)|^2$, where $R(\omega) = \mathrm{e}^{\mathrm{i}kd(n(\omega)-1)}$ is the transmission amplitude in NFSSR. The double-hump structure was used by Smirnov to explain the DB [2]. Since it is discussed in detail elsewhere [54], it is mentioned only briefly here. The direct observation of similar structures in coherent laser spectroscopy has recently been reported [55].

In the double-hump picture, the DB originates from the interference of the frequency components of the two humps. The thicker the sample, the more frequency components far off resonance contribute to the scattering. As a result, the double humps are pushed away from resonance for increasing sample thickness, leading to an increase of the apparent DB frequency.

The double-hump picture has proven to be very useful for a deeper understanding of the DB, in particular in more complicated cases such as for several neighbouring resonances or for distributions of resonances [23,46,47]. Here it is especially important to keep in mind that the double hump relies on scattering rather than on absorption. Therefore interference effects, in particular the destructive interference of the scattering contributions of neighbouring oscillators, strongly influence the appearance of the double hump.

The aperiodicity of the DB, however, and the initial development of NFSSR given by eq. (2.4), are not explained by the time-integral double-hump picture. These features

can only be understood from computed time-differential spectral distributions [2,54]. At very early times, these distributions are of Lorentzian shape, extending over a very broad frequency band. They correspond to the exponential law for the initial time evolution (compare eq. (2.4)). At later times the distribution is transformed into the characteristic double-hump structures, with the separation of the humps decreasing with time. This development can be understood from different scattering times for different frequency components [56]. Scattering at resonance proceeds with the characteristic lifetime t_0. Scattering off resonance, by contrast, is much faster, with the limit of prompt scattering far off resonance. Therefore the off-resonance frequency components die out faster.

4.2. Group-velocity picture

In a region of strong dispersion, in particular near a resonance, the group velocity $v_\mathrm{g} = \mathrm{d}\omega/\mathrm{d}k$ can vary dramatically. For instance, changes in the group velocity of up to almost three orders of magnitude have been observed in investigations of the dispersion relations of exciton-polaritons using pulses of relatively small bandwidth (see [57,58] and references therein). For the transmission of broadband pulses covering the entire resonance, however, the concept of one group velocity for the pulse loses its meaning. Instead, spectral group velocities $v_\mathrm{g}(\omega)$ can be attributed to the different frequency components of the pulse. This concept has proved to be very effective [12,18,20,50,58], and has in particular been employed for the explanation of the polariton beat by Fröhlich et al. [12] as described in the following.

From eq. (2.1) it is seen that around resonance the real part of the dispersion curve $k(\omega) = n(\omega)\omega/c$ is split into two branches, an upper, high-frequency branch (HFB) and a lower, low-frequency branch (LFB). This dispersion relation is sketched in figure 9. In the measurements of the exciton-polariton dispersion mentioned above, the bandwidths of the pulses were usually so small that the polaritons mostly propagated with definite group velocities, corresponding to selected regions on either the HFB or the LFB. But in some cases already the simultaneous excitation of both dispersion branches has been observed [15,57,58]. By contrast, in the propagation of broadband pulses wide regions of both dispersion branches are coherently excited. To each frequency component of the pulse a spectral group velocity $v_\mathrm{g}(\omega) = \mathrm{d}\omega/\mathrm{d}k$ can be attributed, given by the slope of the dispersion curve at the point $k(\omega)$. Note that high (low) spectral group velocities off (near) resonance directly correspond to the short (long) scattering times mentioned before.

After transmission through a sample of thickness d, the intensity measured at time delay t is composed of all frequency components with group velocity $v_\mathrm{g}(\omega) = d/t$. For a narrow, high-frequency resonance, HFB and LFB are practically point-symmetrical with respect to resonance. Thus, for any group velocity $v_\mathrm{g}(\omega)$ two groups of frequency components can be found, one on the HFB, and another on the LFB. These two groups arrive at the same time in the detector and interfere, producing a temporal beat with their difference frequency. From the slopes of the dispersion

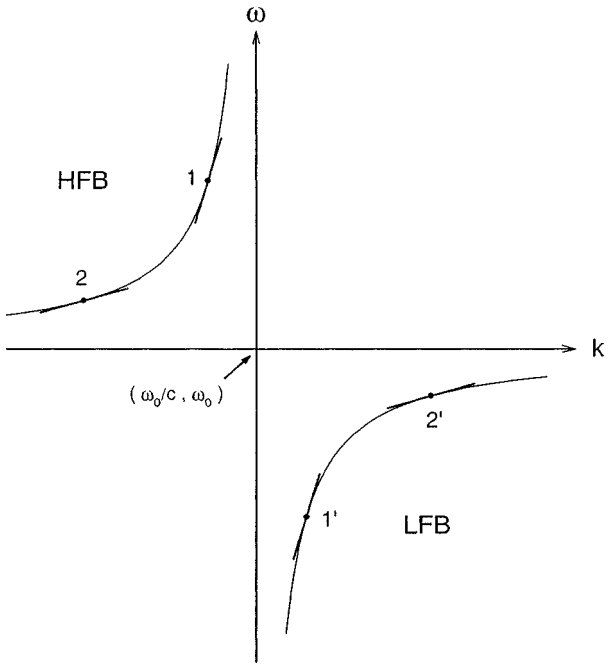

Figure 9. Sketch of a typical dispersion curve near resonance, with damping neglected. The tangents to the two branches of the dispersion curve give the spectral group velocities $v_g(\omega) = d\omega/dk$ for the components of a pulse covering the entire resonance. In the case of a point-symmetrical dispersion curve, two groups of radiation components with the same group velocity are always found, one on the HFB, the other on the LFB. The interference of radiation components with the same high (marked 1, 1′) or low (marked 2, 2′) group velocities results in fast or slow beats, respectively. Since the components with high group velocity arrive first and the slow ones later, RPP through thick samples is characterized by an aperiodic beat with apparent periods increasing in time.

curves it is seen that frequency components far off resonance arrive with high group velocity at early times. Because of their large frequency difference they give rise to fast beats. The opposite holds for the near-resonance frequency components. They arrive with low group velocity at late times, and their small frequency difference gives rise to slow beats. Thus, the aperiodic beat with period increasing in time can be understood as the result of the interference of different frequency components from the two dispersion branches, yielding fast beats at early times and slow beats at late times. In NFSSR, the spectral group velocities cover an extremely large range from $3 \cdot 10^8$ m/s (for the off-resonance components) down to $\sim$10 m/s (e.g., for resonance components arriving after transmission through $\sim$4 μm SS foils with 400 ns delay, compare figure 2(a)).

When the sample thickness is increased, at a fixed delay time radiation components travelling with a higher group velocity and thus separated by a larger frequency difference will arrive. Thus the apparent beat frequency at fixed times will increase with sample tickness as observed in experiments. The group velocity picture is also

corroborated by the fact that the beat is observed only when both dispersion branches are excited, and disappears on detuning [13,48,50]. In particular, the radiation components off resonance will lose their counterparts with the same group velocity on the other side of the resonance. This makes the fast beats observed at early times vanish first upon detuning [48,50].

However, the group-velocity picture has an important disadvantage: it is not obvious with which strength the different frequency components are actually scattered. Here one has to keep in mind first of all the $1/(\omega - \omega_0)$ dependence of the resonance scattering amplitude for an individual scatterer (see eq. (2.1)). For this reason the scattering of the off-resonance frequency components is in general less intense than that of the near-resonance components, so that the off-resonance parts of the dispersion branches contribute less than the near-resonance parts. In addition, multiple scattering in an ensemble of scatterers completely rearranges the contributions of the different frequency components. For example, in resonance scattering by a thick sample certain frequency regions above and below resonance become dominant and form the time-dependent double-hump structures mentioned above [2,54]. Moreover, in a thin sample and also for the very first moments in a thick sample, the contributions from wide regions of the dispersion branches build up a broad and smooth Lorentzian frequency distribution, which corresponds to the exponential decay given by eq. (2.4). These features are not obvious from the group-velocity picture.

4.3. Coupled-system picture

The pictures discussed so far were developed in order to interpret the features of RPP with the help of intermediate constructions like double humps or dispersion curves. However, they do not yet convey an understanding of the physical origin of the effects of RPP.

The origin of the beat phenomena observed in RPP has been pointed out by Burnham and Chiao [8]. They demonstrate that the radiation field envelope is the time-derivative of the atomic polarization envelope. This relation leads to a shift of $\pi/2$ between the oscillatory time evolutions of the radiation field and of the atomic polarization (compare [8, figure 2]). Such a behaviour is characteristic for a coupled system which exchanges energy, for instance two weakly coupled harmonic oscillators. It is, therefore, straightforward to interpret the radiation field, the envelope of which exhibits the characteristic ringing described by eqs. (2.2) and (2.3), as one partner of a coupled system. In NFS of Mössbauer radiation or SR this coupled system consists of the radiation field and the nuclear polarization (or nuclear currents).

A crucial point is the coupling strength of the energy exchange, which is expected to determine the beat frequency. Burnham and Chiao have shown the coupling to be proportional to the coherent scattering strength of the oscillators, which is given by ω_p^2 (compare [8, eq. (13)]) or, more generally, by the parameter a^2 in eq. (2.1). As a consequence, the modulation of the transmitted pulse in space and time is determined

by the strength of the oscillators, and not by their lifetime t_0, as could be inferred for instance from considerations like those given at the beginning of section 4. This is obvious in the off-resonance notation, where the argument under the square root of the Bessel function $(\omega_p^2/c)td$ [8] or its quantum-optical analog $4\alpha_0 td$ [9] does not contain the oscillator lifetime, and where a Bessel modulation can also be derived in the approximation of infinite oscillator lifetimes [8,48]. In the in-resonance notation the oscillator strength is given by c times the absorption area $\mu_r\Gamma_0/\hbar = T/t_0 d$. Thus, a change of the oscillator lifetime t_0 leaves the Bessel modulation unaffected, as long as the absorption area remains constant. A good example is the case of Lorentzian line-broadening, which leaves the absorption area and, thus, the Bessel modulation unchanged and causes only a faster decay of the signal [23].

The rate of energy interchange is proportional to the product of field strength and nuclear polarization. But since the nuclear polarization itself is induced by the radiation field, the exchange rate becomes proportional to the total energy stored. Therefore, the coupling is weaker and the beat frequency is lower for thinner samples, where less energy had been extracted from the SR pulse. Also, the increase of the apparent beat period with time can be understood in these terms [8]: after the initial collective nuclear excitation, energy is flowing out of the sample by reemission of radiation, and therefore the radiative coupling and the resulting frequency of the energy exchange are decreasing with time.

It is important to keep in mind that the exchange between nuclear polarization energy and radiation field energy depends both on time and space. Formally, this is expressed by the fact that normalized time τ and effective thickness T appear only as a product $T\tau$ in the argument of the Bessel functions of eqs. (2.2) and (2.3). At the same time there are regions at different depths in the sample where the energy exchange shifts the energy predominantly into the polarization, and other regions where the energy is in the field. This causes the radiation to arrive in bunches as it leaves the sample.

At time zero, when the nuclear ensemble is excited by the SR pulse, both the radiation field and the nuclear polarization are at a maximum. The onset of the subsequent energy exchange between field and polarization is characterized by an initial strong decrease of both radiation field and nuclear polarization because of radiation flowing out of the sample (compare [8, figure 2]). The fast decay of the radiation field, often referred to as speed-up of the initial decay, can be understood as a transient effect initiating the subsequent beating phenomena. It has been interpreted as being due to an enhancement of the coherent channel in resonant scattering by an ensemble of oscillators. For such collective excitation states in nuclear resonant Bragg scattering and forward scattering of Mössbauer radiation or SR, strongly enhanced superradiant decay rates have been predicted in theoretical investigations by the groups of Trammell and Hannon, and of Kagan and Afanas'ev (for further discussion and references see [59, 60]).

5. Discussion

5.1. Universality of the phenomena

It is remarkable that the observed phenomena of RPP are quite universal, both with respect to the wavelength of the radiation and with respect to the type of resonance and resonant medium. The characteristic features of RPP as defined in section 3.3 are observed in many fields of radiation physics.

Features of RPP have been observed in the wavelength range $\lambda \approx 1$ Å–1 m, from γ-radiation to microwaves. This lack of sensitivity of a coherent phenomenon to the wavelength is at first surprising. But it is immediately explained by the fact that in the forward direction the spatial scattering phases are always constructive. Therefore, the scattering is spatially coherent, independent of the ratio between wavelength and spatial separation of the scattering centers. Spatial coherence in forward scattering can be demonstrated by interresonance interference, when many-atom quantum beats [61] are observed in scattering from different nuclear [6,22] or molecular [51,52] scattering centers of slightly different resonance energies. However, in the case of a single resonance already, spatial coherence becomes manifest in the effects of RPP.

In the presence of dynamics, however, the wavelength plays a decisive role. When the scattering centers are displaced during the characteristic scattering time, the forward scattering may be perturbed. Vibrational elongations produced by ultrasound of 15 MHz, for instance, can easily become comparable to the wavelength of ^{57}Fe γ-radiation (0.086 nm) in the time window of nuclear scattering (lifetime 141 ns), leading to a temporal destruction of the constructive interference [62]. By contrast, in molecular gases [10,51,52] and in atomic vapors [11,48,53] the displacements during the short relaxational dephasing times in the range of 1–100 ps are very small in comparison with the long wavelengths in the infrared and visible regimes. Therefore, effects relying on spatial coherence like many-atom quantum beats or pulse propagation beats can be observed even in gases and vapors. In these experiments, the spatial dephasing due to translational motion can usually be neglected in comparison with relaxational dephasing due to collisions.

The wavelength or the energy of the radiation also plays a role with respect to the physical state of the resonant medium. RPP is a coherent phenomenon and relies on elastic, recoilfree scattering in order to make the different scattering paths indistinguishable. For γ-radiation the resonant medium has to be a solid with non-vanishing Lamb–Mössbauer factor in order to observe RPP. For low energy radiation in the visible or infrared, by contrast, the recoil shift is much smaller than the natural linewidth, and the forward scattering is coherent in liquids [63] and in gases [51] or vapors [11,48] as well.

The features of RPP also seem to be independent of the particular type of resonance. Especially there is no serious difference between two-level resonances (nuclear, atomic and bound-excitonic) and lattice excitations (free excitons, transverse optical phonons). Two-level resonances are individual resonances, which become coupled only via the radiation field. The coupling leads to a polariton-like state of collective,

delocalized excitation, which comprises radiation and resonant system. In the case of nuclear scattering this state is called a nuclear exciton. Lattice excitations, by contrast, are themselves already collective excitations with spatial dispersion. The additional coupling with the radiation field leads to mixed states known as exciton–polariton or phonon-polariton, respectively. However, since the dispersion of the lattice excitations is very small in the narrow region of crossover with the steep photon dispersion curve, the dispersion branches described by eq. (2.1) and thus the effects of RPP altogether are not much influenced by spatial dispersion [12,50].

Finally, we want to point out that oscillatory time evolutions with periods increasing with time, which are described by Bessel- or cos-functions of argument $\sqrt{T\tau}$, respectively $\sqrt{a^2 t\, d/c}$, occur, to our knowledge, only in RPP. Thus, they can be considered as a unique fingerprint of RPP.

5.2. Mutual stimulations

Besides the general interest in universal phenomena, we may ask how areas in physics where such widely different wavelengths and such different types of resonances are used, can profit from each other. First let us see what the field of NFSSR could learn from the physics of RPP in the visible region.

Due to the limited brilliance of SR sources, NFSSR has so far been observed in single photon excitation and in the linear regime. Even at a third generation SR source like ESRF, less than one nuclear excitation happens per 100 lifetimes of ^{57}Fe. However, NFSSR in the nonlinear regime could become possible at future X-ray sources. Optical studies using laser sources, by contrast, can easily be extended to the nonlinear regime. Here experience has been gained by experiments on RPP in the transition from the linear to the nonlinear regime [13,14,64–66]. Moreover, the theoretical description of nonlinear phenomena has been developed for laser radiation in the infrared and visible (see, e.g., [16] and references therein).

NFS can so far be performed only with radiation sources, where the ratio Q of the energy widths of pulse to resonance is either unity (radioactive source) or of order 10^5–10^6 (SR). With laser sources and resonances in the visible, by contrast, ratios Q between these limits are realized, with typical values $Q \approx 10$–100. Lower width ratios would be a great help in NFSSR in order to decrease the extreme load on detector and detector curcuit by the prompt pulse. Ultra-monochromatization by nuclear broadband-filtering [67] could be a solution to the problem. Such ultra-monochromatization would lead to conditions comparable to those prevailing with laser sources. Mathematical expressions for the time evolution of NFS have meanwhile been derived for arbitrary ratios Q_{L} of Lorentzian pulse and resonance widths [68].

From the technical point of view, optical devices for visible light like Michelson interferometers [14] or high-finesse Fabry–Perot cavities [55] are a permanent challenge for the γ-radiation regime. First steps towards the development of such devices for γ-radiation have recently been reported [69].

Finally, NFSSR can profit from the ideas and concepts developed in the field of resonant propagation of laser pulses. Good examples here are the group velocity interpretation of the polariton beat [12] and the energy exchange between radiation field and oscillator system [8] described in sections 4.2 and 4.3.

On the other hand, the developments of NFSSR could also be of interest for the visible region. Nuclear resonances are in many ways ideal oscillators, which perfectly represent the concept of a two-level system [16]. They are strong resonators, corresponding in the case of ^{57}Fe, e.g., to several hundreds of electrons with respect to scattering power. In contrast to the common situation with molecular, atomic and excitonic resonances, they are completely isolated in energy. They exhibit well-known properties of hyperfine splitting in electric or magnetic fields and of polarization dependence. For the RPP of γ-radiation both from radioactive sources and from SR sources closed analytical solutions exist (eqs. (2.2) and (2.3)). These expressions allow a fast direct verification of the experimental results in the visible also, for instance by checking the positions of the minima of the observed beat.

The nuclear resonance of ^{57}Fe has a lifetime of 141 ns, which is very long compared to lifetimes in the visible. This allows application of external perturbations to the collective excitation. Coherent transient phenomena after external perturbations of the absorber like, e.g., fast magnetization inversion or spatial shifts had been studied since long in NFS of Mössbauer radiation (see, e.g., [35,36] and references therein). In NFSSR, perturbations by ultrasound vibrations [62,70–73] and by fast switching of the magnetization [74] have so far been studied.

The extremely narrow linewidth connected with the long lifetime allows one to Doppler shift the resonance continuously by up to hundreds of linewidths. This sensitivity facilitates interesting experiments. For instance, it allows investigating a problem also known in the visible regime, the combination of RPP and interresonance interference. Interresonance interference is used in molecular [51], atomic [61], excitonic [75] and nuclear [1,76] quantum beat spectroscopy to determine resonance line separations. In optically thick samples, however, the interference of quantum beat and propagation beat leads to serious complications [23,65,77,82]. In NFSSR, the influence of interresonance interference on RPP can be studied systematically by Doppler shifting resonance lines. For this purpose, e.g., one of two identical targets mounted downstream behind the other can be moved with constant Doppler velocity, thus simulating a variable two-line quadrupole splitting [46,47]. In similar model experiments the effect of radiative coupling between two resonances of different linewidth on RPP can be investigated [78]. Such external perturbations during the excited state lifetime or similar model experiments using resonant line shifts via the Doppler effect are practically impossible with the short-lived, broad resonances in the visible region.

Nuclear resonant scattering also has a strong incoherent scattering channel due to internal conversion, which leads, e.g., in the case of the 14.4 keV transition of ^{57}Fe to the emission of conversion electrons and characteristic 6.4 keV X-radiation. When this radiation is recorded at a certain depth in the target, the nuclear polarization is probed at this place. The nuclear polarization (or nuclear currents) is the

counterpart of the radiation field in the energy exchange between field and nuclear oscillators. Thus the energy exchange described in section 4.3 can be investigated by the simultaneous measurement of the coherent and incoherent nuclear scattering channels. In practice, however, such studies are limited to very thin samples because of a competing nonresonant scattering channel. Except for very thin foils, incoherent scattering by the photoeffect, which directly reflects the radiation field intensity, dominates the nuclear incoherent channel via internal conversion, which reflects the nuclear polarization [40,79–81].

The characteristic DB in the case of a Lorentzian oscillator depends only on the effective thickness T and on the lifetime t_0 (compare eq. (2.3)). Both values can be retrieved from the time evolution, with T containing specific information on the strength of the oscillator and the density of the oscillators in the sample. For light scattering by excitonic resonances, for instance, the propagation beat was used for an accurate determination of the involved oscillator strengths [12]. In the case of γ-ray scattering by nuclear resonances, the coherent scattering strength depends on the reduction factor for recoilfree scattering, which in NFS is equivalent to the standard Lamb–Mössbauer factor f_{LM}. Thus the pronounced DB in NFSSR in principle allows an easy and precise determination of a key parameter of Mössbauer spectroscopy [1,39]. However, in the case of several neighbouring resonances caused, e.g., by hyperfine splitting, the DB is usually affected by interresonance interference [23,46,47,82]. Then the precision of the Lamb–Mössbauer factor determined from the DB depends on the accuracy of the knowledge of the hyperfine interactions.

6. Summary

The characteristic features of pulse propagation of SR through nuclear resonant samples have been described. An astonishing universality of the phenomena observed in RPP has been revealed by a comparison with RPP in the infrared and visible region in the case of molecular, atomic and excitonic resonances. The origin of the most prominent feature, the DB, has been interpreted in the double-hump picture and in the group-velocity picture and has finally been ascribed to an energy exchange between radiation field and oscillator system. Possibilities of mutual stimulation between the γ-radiation and the visible-light regimes with respect to research on RPP have been discussed.

Acknowledgements

The work has been supported by the Bundesministerium für Bildung, Wissenschaft, Forschung und Technologie under Contract No. 643WOA. The author would like to thank Yu.V. Shvyd'ko, D. Fröhlich, M. Rosenbluh and A. Laubereau for kindly allowing the reproduction of figures 2, 6, 7 and 8, respectively. The author also gratefully acknowledges extensive critical and stimulating discussions with G.V. Smirnov, W. Potzel and Yu.V. Shvyd'ko.

References

[1] E. Gerdau and U. van Bürck, in: *Resonant Anomalous X-Ray Scattering*, eds. G. Materlik, C.J. Sparks and K. Fischer (Elsevier Science, Amsterdam, 1994) p. 589;
U. van Bürck and G.V. Smirnov, Hyp. Interact. 90 (1994) 313.

[2] G.V. Smirnov, Hyp. Interact. 97/98 (1996) 551; in: *X-Ray and Inner-Shell Processes*, eds. R.L. Johnson, H. Schmidt-Böcking and B.F. Sonntag, AIP Conf. Proc. 389 (AIP, New York, 1997) p. 323.

[3] A. Sommerfeld, Ann. Phys. 44 (1914) 177;
L. Brillouin, Ann. Phys. 44 (1914) 203; and *Wave Propagation and Group Velocity* (Academic Press, New York, 1960).

[4] F.J. Lynch, R.E. Holland and M. Hamermesh, Phys. Rev. 120 (1960) 513;
R.E. Holland, F.J. Lynch, G.J. Perlow and S.S. Hanna, Phys. Rev. Lett. 4 (1960) 181.

[5] E. Gerdau, R. Rüffer, H. Winkler, W. Tolksdorf, C.P. Klages and J.P. Hannon, Phys. Rev. Lett. 54 (1985) 835.

[6] J.B. Hastings, D.P. Siddons, U. van Bürck, R. Hollatz and U. Bergmann, Phys. Rev. Lett. 66 (1991) 770.

[7] Yu. Kagan, A.M. Afanas'ev and V.G. Kohn, J. Phys. C: Solid State Phys. 12 (1979) 615.

[8] D.C. Burnham and R.Y. Chiao, Phys. Rev. 188 (1969) 667.

[9] M.D. Crisp, Phys. Rev. A 1 (1970) 1604.

[10] H.J. Hartmann and A. Laubereau, Opt. Commun. 47 (1983) 117.

[11] J.E. Rothenberg, D. Grischkowsky and A.C. Balant, Phys. Rev. Lett. 53 (1984) 552.

[12] D. Fröhlich, A. Kulik, B. Uebbing, A. Mysyrowicz, V. Langer, H. Stolz and W. von der Osten, Phys. Rev. Lett. 67 (1991) 2343.

[13] M. Jütte, H. Stolz and W. von der Osten, Phys. Status Solidi B 188 (1995) 327; J. Opt. Soc. Amer. B 13 (1996) 1205;
M. Jütte, thesis, University of Paderborn (1997).

[14] D.S. Kim, J. Shah, D.A.B. Miller, T.C. Damen, W. Schäfer and L. Pfeiffer, Phys. Rev. B 48 (1993) 17902;
D.S. Kim, J. Shah, D.A.B. Miller, T.C. Damen, A. Vinaretti, W. Schäfer and L.N. Pfeiffer, Phys. Rev. B 50 (1994) 18240.

[15] H.J. Bakker, S. Hunsche and H. Kurz, Phys. Rev. Lett. 69 (1992) 2823; Phys. Rev. B 48 (1993) 13524 and 50 (1994) 914; Rev. Mod. Phys. 70 (1998) 523.

[16] L. Allen and J.H. Eberly, *Optical Resonance and Two-Level Atoms* (Wiley, New York, 1975);
G.L. Lamb, Jr., Rev. Mod. Phys. 43 (1971) 99.

[17] U. van Bürck and G.V. Smirnov, in: *ICAME 1995, Book of Abstracts*, p. 12-22.

[18] J.A. Stratton, *Electromagnetic Theory* (McGraw-Hill, New York, 1941) section 5.18;
J.D. Jackson, *Classical Electrodynamics*, 2nd ed. (Wiley, New York, 1975) sections 7.10–11.

[19] K.E. Oughstun and C.M. Balictsis, Phys. Rev. Lett. 77 (1996) 2210.

[20] P. Pleshko and I. Palócz, Phys. Rev. Lett. 22 (1969) 1201.

[21] S.M. Harris, Phys. Rev. 124 (1961) 1178.

[22] U. van Bürck, D.P. Siddons, J.B. Hastings, U. Bergmann and R. Hollatz, Phys. Rev. B 46 (1992) 6207.

[23] Y.V. Shvyd'ko, U. van Bürck, W. Potzel, P. Schindelmann, E. Gerdau, O. Leupold, J. Metge, H.D. Rüter and G.V. Smirnov, Phys. Rev. B 57 (1998) 3552.

[24] A. Laubereau and W. Kaiser, Rev. Mod. Phys. 50 (1978) 607.

[25] S.L. Ruby, unpublished; see [70].

[26] G.R. Hoy, J. Phys.: Condens. Matter 9 (1997) 8749;
G.R. Hoy, J. Odeurs and R. Coussement, Hyp. Interact. C 3 (1998) 425.

[27] Y.V. Shvyd'ko, Phys. Rev. B 59 (1999) 9132; and this issue, section III-1.3.

[28] M. Haas, V. Hizhnyakov, E. Realo and J. Jögi, Phys. Status Solidi B 149 (1988) 283.

[29] J. Aaviksoo, J. Kuhl and K. Ploog, Phys. Rev. A 44 (1991) R5353.

[30] N. Hayashi, T. Kinoshita, I. Sakamoto and B. Furubayashi, Nucl. Instrum. Methods 134 (1976) 317.
[31] E.I. Vapirev, P.S. Kamenov, D.L. Balabanski, S.I. Ormandjiev and K. Yanakiev, J. Phys. 44 (1983) 675.
[32] C.S. Wu, Y.K. Lee, N. Benczer-Koller and P. Simms, Phys. Rev. Lett. 5 (1960) 432.
[33] M. Alflen, C. Hennen, F. Tuczek, H. Spiering, P. Gütlich and Z. Kajcsos, Hyp. Interact. 47 (1989) 115.
[34] E. Ikonen, P. Helistö, T. Katila and K. Riski, Phys. Rev. A 32 (1985) 2298.
[35] P. Helistö, E. Ikonen and T. Katila, Phys. Rev. B 34 (1986) 3458;
I. Tittonen, M. Lippmaa, P. Helistö and T. Katila, Phys. Rev. B 47 (1993) 7840.
[36] Y.V. Shvyd'ko, S.L. Popov and G.V. Smirnov, J. Phys.: Condens. Matter 5 (1993) 1557.
[37] Y.V. Shvyd'ko, G.V. Smirnov, S.L. Popov and T. Hertrich, JETP Lett. 53 (1991) 69.
[38] S. Kikuta, in: *Resonant Anomalous X-Ray Scattering*, eds. G. Materlik, C.J. Sparks and K. Fischer (Elsevier Science, Amsterdam, 1994) p. 635.
[39] U. Bergmann, S.D. Shastri, D.P. Siddons, B.W. Batterman and J.B. Hastings, Phys. Rev. B 50 (1994) 5957.
[40] J. Arthur, G.V. Smirnov, U. van Bürck, S.L. Ruby, A.Q.R. Baron, A.I. Chumakov and G.S. Brown, in: *ICAME 1995, Book of Abstracts*, p. 12-32.
[41] Y.V. Shvyd'ko, unpublished.
[42] U. van Bürck, W. Potzel, P. Schindelmann, E. Gerdau, Y.V. Shvyd'ko, O. Leupold and H.D. Rüter, HASYLAB, Ann. Report (1998) 955.
[43] Y. Hasegawa, Y. Yoda, K. Izumi, T. Ishikawa, S. Kikuta, X.W. Zhang and M. Ando, Phys. Rev. B 50 (1994) 17748.
[44] U. van Bürck, W. Potzel, P. Schindelmann, G.V. Smirnov, S.L. Popov, E. Gerdau, O. Leupold, Y.V. Shvyd'ko and H.D. Rüter, HASYLAB, Ann. Report (1996) 884.
[45] G.V. Smirnov, S.L. Popov, U. van Bürck, W. Potzel, P. Schindelmann, E. Gerdau, O. Leupold, Y.V. Shvyd'ko and H.D. Rüter, HASYLAB, Ann. Report (1996) 890.
[46] U. van Bürck, W. Potzel, P. Schindelmann, G.V. Smirnov, E. Gerdau, O. Leupold, Y.V. Shvyd'ko and H.D. Rüter, HASYLAB, Ann. Report (1997) 939.
[47] Y.V. Shvyd'ko and U. van Bürck, this issue, section IV-2.2.
[48] M. Matusovsky, B. Vaynberg and M. Rosenbluh, J. Opt. Soc. Amer. B 13 (1996) 1994.
[49] T. Mishina and Y. Masumoto, Phys. Rev. Lett. 71 (1993) 2785.
[50] S. Nüsse, P.H. Bolivar, H. Kurz, F. Levy, A. Chevy and O. Lang, Phys. Rev. B 55 (1997) 4620.
[51] H.J. Hartmann, K. Bratengeier and A. Laubereau, Chem. Phys. Lett. 108 (1984) 555.
[52] H.J. Hartmann and A. Laubereau, J. Chem. Phys. 80 (1984) 4663.
[53] O. Kinrot and Y. Prior, Phys. Rev. A 51 (1995) 4996 and 50 (1994) R1999.
[54] G.V. Smirnov, this issue, section II-2.
[55] J.K. Ranka, R.W. Schirmer and A.L. Gaeta, Phys. Rev. A 57 (1998) R36.
[56] G.V. Smirnov and Y.V. Shvyd'ko, Sov. Phys. JETP 68 (1989) 444.
[57] Y. Masumoto, Y. Unuma, Y. Tanaka and S. Shionoya, J. Phys. Soc. Japan 47 (1979) 1844;
R.G. Ulbrich and G.W. Fehrenbach, Phys. Rev. Lett. 43 (1979) 963;
S. Chu and S. Wong, Phys. Rev. Lett. 48 (1982) 738.
[58] T. Itoh, P. Lavallard, J. Reydellet and C. Benoit, Solid State Commun. 37 (1981) 925.
[59] J.P. Hannon and G.T. Trammell, in: *Resonant Anomalous X-Ray Scattering*, eds. G. Materlik, C.J. Sparks and K. Fischer (Elsevier Science, Amsterdam, 1994) p. 565; this issue, section III-1.2.
[60] Yu. Kagan, this issue, section III-1.1.
[61] S. Haroche, in: *High-Resolution Laser Spectroscopy*, ed. K. Shimoda (Springer, Berlin, 1976) p. 253.
[62] G.V. Smirnov, U. van Bürck, J. Arthur, S.L. Popov, A.Q.R. Baron, A.I. Chumakov, S.L. Ruby, W. Potzel and G.S. Brown, Phys. Rev. Lett. 77 (1996) 183.
[63] R. Laenen and A. Laubereau, Opt. Commun. 101 (1993) 43.
[64] M. Matusovsky, B. Vaynberg and M. Rosenbluh, Phys. Rev. Lett. 77 (1996) 5198.

[65] U. Neukirch, K. Wundke, J. Gutowski and D. Hommel, Phys. Status Solidi B 196 (1996) 473.
[66] U. Neukirch and K. Wundke, Phys. Rev. B 55 (1997) 15408.
[67] R. Röhlsberger, E. Gerdau, R. Rüffer, W. Sturhahn, T.S. Toellner, A.I. Chumakov and E.E. Alp, Nucl. Instrum. Methods A 394 (1997) 251;
R. Röhlsberger, this issue, section IV-1.3.
[68] G.C. Baldwin, Nucl. Instrum. Methods 159 (1979) 309;
G.J. Perlow, Hyp. Interact. 72 (1992) 51.
[69] Y.V. Shvyd'ko, E. Gerdau, J. Jäschke, O. Leupold, M. Lucht and H.D. Rüter, Phys. Rev. B 57 (1998) 4968.
[70] T. Mitsui, T. Shimizu, Y. Imai, Y. Yoda, X.W. Zhang, H. Takei, T. Harami and S. Kikuta, Japan. J. Appl. Phys. 36 (1997) 6525; Hyp. Interact. C 3 (1998) 429.
[71] H. Jex, A. Ludwig, F.J. Hartmann, E. Gerdau and O. Leupold, Europhys. Lett. 40 (1997) 317;
A. Ludwig and H. Jex, Phys. B 254 (1998) 1.
[72] G.V. Smirnov and W. Potzel, this issue, section IV-2.8.
[73] P. Schindelmann, W. Potzel, U. van Bürck, G.V. Smirnov, S.L. Popov, E. Gerdau, Y.V. Shvyd'ko and H.D. Rüter, HASYLAB, Ann. Report (1998) 951.
[74] Y.V. Shvyd'ko, T. Hertrich, U. van Bürck, E. Gerdau, O. Leupold, J. Metge, H.D. Rüter, S. Schwendy, G.V. Smirnov, W. Potzel and P. Schindelmann, Phys. Rev. Lett. 77 (1996) 3232.
[75] W. von der Osten, V. Langer and H. Stolz, in: *Coherent Optical Interactions in Semiconductors*, ed. R.T. Phillips (Plenum, New York, 1994) p. 111;
K.H. Pantke and J.M. Hvam, Internat. J. Modern Phys. B 8 (1994) 73.
[76] G.T. Trammell and J.P. Hannon, Phys. Rev. B 18 (1978) 165 and 19 (1979) 3835.
[77] D. Fröhlich, A. Kulik, B. Uebbing, V. Langer, H. Stolz and W. von der Osten, Phys. Status Solidi B 173 (1992) 31.
[78] W. Potzel, U. van Bürck, P. Schindelmann, G.V. Smirnov, E. Gerdau, Y.V. Shvyd'ko and H.D. Rüter, HASYLAB, Ann. Report (1998) 953.
[79] U. Bergmann, J.B. Hastings and D.P. Siddons, Phys. Rev. B 49 (1994) 1513.
[80] G.V. Smirnov and V.G. Kohn, Phys. Rev. B 52 (1995) 3356.
[81] W. Sturhahn, K.W. Quast, T.S. Toellner, E.E. Alp, J. Metge and E. Gerdau, Phys. Rev. B 53 (1996) 171.
[82] M. Haas, E. Realo, H. Winkler, W. Meyer-Klaucke, A.X. Trautwein, O. Leupold and H.D. Rüter, Phys. Rev. B 56 (1997) 14082.
[83] Motif, a program based on [27] available from the anonymous `ftp://i2aix04.desy.de/pub/motif` or from the author via e-mail `Yuri.Shvydko@desy.de`.